Proc. NIPR Symp. Upper Atmos. Phys., **12**, 30–38, 1998

SIMULTANEOUS OBSERVATIONS OF THE AURORA AND OF NON-UNIFORM THERMOSPHERIC WINDS, FROM POKER FLAT, ALASKA

Mark CONDE and Roger W. SMITH

Geophysical Institute, University of Alaska, 903 Koyukuk Drive, P. O. Box 757320, Fairbanks, Alaska 99775-7320, U.S.A.

Abstract: A new all-sky imaging, wavelength scanning Fabry-Perot spectrometer (FPS) has been developed to spatially resolve horizontal vector wind fields in the thermosphere approximately 240 km above Poker Flat, Alaska. Collocated with this instrument are a narrow field Fabry-Perot spectrometer, a 30 frame/s white light all-sky video camera (ASC) and a 4-channel meridian scanning photometer (MSP). The narrow field FPS is normally used for vertical wind measurements, whereas the latter two instruments are used to monitor auroral activity. We present an example of data from this set of instruments from one night, November 15, 1996. In particular, we focus on a three hour period, ending just after magnetic midnight, during which time an auroral breakup was observed. Strong curvature and shear of the horizontal wind field developed prior to the breakup, apparently associated with stable aurora lying north of Poker Flat. The curved and sheared flow configuration collapsed within 45 min of the breakup, leaving the thermospheric wind almost stagnant. Following this, the observatory moved under the thermospheric cross-polar jet, so that uniform southeastward wind gradually covered our visible sky. The vertical wind speed remained within a few tens of ms^{-1} of zero throughout this period, apart from an isolated value of 82 ms^{-1} downward, recorded about 50 min prior to the breakup. Mechanisms for possible associations between thermospheric vertical winds, horizontal winds, and the aurora are discussed.

1. Introduction

Numerous publications of thermospheric neutral wind data have shown strong velocity shears in the horizontal wind at high latitude (*e.g.* SPENCER *et al.*, 1982; HAYS *et al.*, 1984; KILLEEN *et al.*, 1988). The global-scale relationship between thermospheric winds and auroral morphology has been examined extensively by KILLEEN *et al.* (1988). A principal outcome of this study was to demonstrate the close association between reversals and boundaries in the neutral wind and the location of the aurora. High spatial resolution atmospheric models also predict that strong shears may develop in the thermospheric wind field within several hundred km of an auroral arc (ST.-MAURICE and SCHUNK, 1981; FULLER-ROWELL, 1985; LYONS and WALTERSCHEID, 1985; WALTERSCHEID *et al.*, 1985; CHANG and ST.-MAURICE, 1991; WALTERSCHEID and LYONS, 1992; KESKINEN and SATYANARAYANA, 1993).

Thermospheric winds have been measured above interior Alaska previously using ground-based Fabry-Perot spectrometers (NAGY *et al.*, 1974; HAYS *et al.*, 1979; SICA *et al.*, 1986, 1989, 1993; SMITH *et al.*, 1989), rocket-borne chemical releases (MERIWETHER *et al.*, 1973; MIKKELSEN *et al.*, 1981; HEPPNER and MILLER, 1982;

LARSEN *et al.*, 1995, 1997), incoherent scatter radar (BATES and ROBERTS, 1977; WICKWAR *et al.*, 1984) and by the Dynamics Explorer 2 satellite (*e.g.* KILLEEN and ROBLE, 1988).

These measurements have returned little detailed information about the spatial variation of the horizontal wind. Neither rocket-borne chemical releases nor the 5-direction FPI experiments have provided enough information to uniquely estimate all of the terms required to describe even first order departures from a uniform horizontal wind vector field. Dynamics Explorer 2 was able to measure wind variations along one direction, *i.e.* aligned with its orbital track. However, it was neither able to determine the two-dimensional spatial variation of the horizontal vector wind field, nor could it follow the evolution of this field with time above a fixed geographic position.

2. Instrumentation

All of the observations reported here were taken from Poker Flat, Alaska. This site is located geographically at 65°07′ north, 147°26′ west, and its magnetic latitude is 64°57′ north. The wind observations were obtained during winter-time solar minimum conditions using both an all-sky imaging Fabry-Perot spectrometer (ASI-FPS) and a narrow field imaging FPS. The wind measurements were derived from Doppler shifts of the λ630 nm optical emission from atomic oxygen, originating at $\sim$240 km altitude.

The ASI-FPS instrument used in the present study (described by CONDE and SMITH, 1997) encodes spectral information by scanning the etalon plate spacing over time. Because the etalon scan is independent of the spatial distribution of luminosity, this instrument is unaffected by spatial intensity gradients associated with the aurora. For the observations described here, we divided the ASI-FPS field-of-view into 25 "zones" mapping onto the sky as sectors of four concentric, annular, rings centered about the zenith. The ring edges were spaced uniformly in zenith angle, with the outermost being at 65°. The rings contained 1, 4, 8 and 12 azimuthal sectors respectively. The procedure used to infer the horizontal vector wind field from the ASI-FPS data (which are solely line-of-sight measurements) has been described by CONDE and SMITH (1998).

The all-sky camera (ASC) is a broad-band (white light) intensified CCD video system viewing a 180° full-angle field-of-view at 30 frames per second. The meridian scanning photometer (MSP) records the distribution of auroral luminosity along the magnetic meridian, using a rotating mirror to sweep the $\sim$1° (full angle) fields-of-view of four-narrow band photometers. Each complete mirror rotation takes 4 s, with the sky being observed for half this time. The photometer interference filters are re-tuned (by tilting) between the sky observing times to alternately transmit "on-wavelength" and "off-wavelength" for the emission lines of interest. In this way, every second sky scan yields an estimate of any continuum background that may be superimposed on the auroral or airglow emission lines. The data presented here were obtained by adding pairs of two successive on-wavelength scans and subtracting the corresponding pair of off-wavelength scans, with the resulting total time interval being 16 s.

3. Observations and Discussion

The instrumentation was operated from mid October through early May of the 1996/97 northern winter. The sky conditions (*i.e.* extent and nature of cloud cover) were assessed using a combination of data from all instruments, although the ASC and MSP gave the best indications. The data presented here are from the night of November 15, 1996. We chose this night for three reasons, *i.e.* it was clear and moonless, all instruments were observing simultaneously and operating well, and the thermospheric wind fields which we observed are representative of a pattern that occurred frequently during the 1996/97 season (on at least one third of all nights).

The geomagnetic A_p index for November 15, 1996, was 11 and the $F_{10.7}$ solar radio flux index was 74. The IMF B_z component was variable within ± 6 nT whereas the IMF B_y component was a few nT positive before 08 UT, but up to 20 nT positive after 08 UT. Complete time-series plots of the IMF values for this day can be made from the data returned by the MFI instrument aboard the WIND spacecraft.

The format of the wind vector and ASC plots presented here is such that geomagnetic north is at the top and geomagnetic east is at the right, as would be seen by an observer looking down on the Earth. However, note that neither the wind nor camera plots have been projected to a spatial coordinate system. This means that radial distance from the center in these plots maps linearly to observing zenith angle, rather than to horizontal distance. It should also be noted that the ASC and ASI-FPS fields of view were slightly different. The ASC viewed a 180° full-angle field-of-view, whereas the

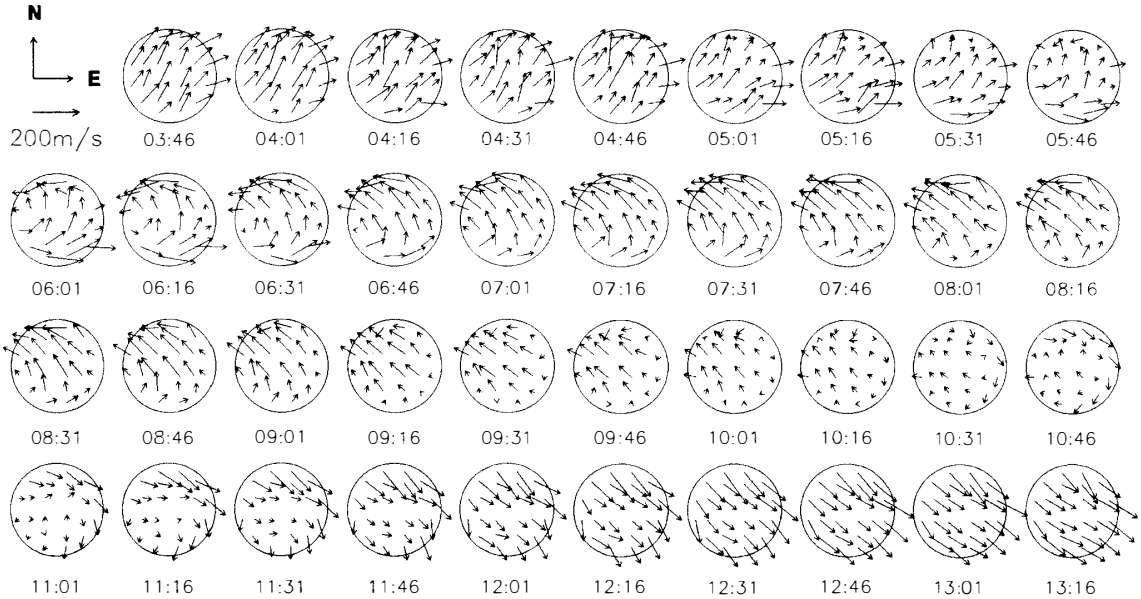

Fig. 1. Evolution of the thermospheric horizontal vector wind field on the night of the November 15, 1996, shown at 15 min intervals. Geomagnetic north is at the top and geomagnetic east is at the right, as would be seen by an observer looking down on the Earth. However, note that the wind vectors have not been projected to a spatial coordinate system. This means that radial distance from the center of each plot maps linearly to observing zenith angle, rather than to horizontal distance. The arrow labelled 200 ms $^{-1}$ at the top left indicates the velocity scale.

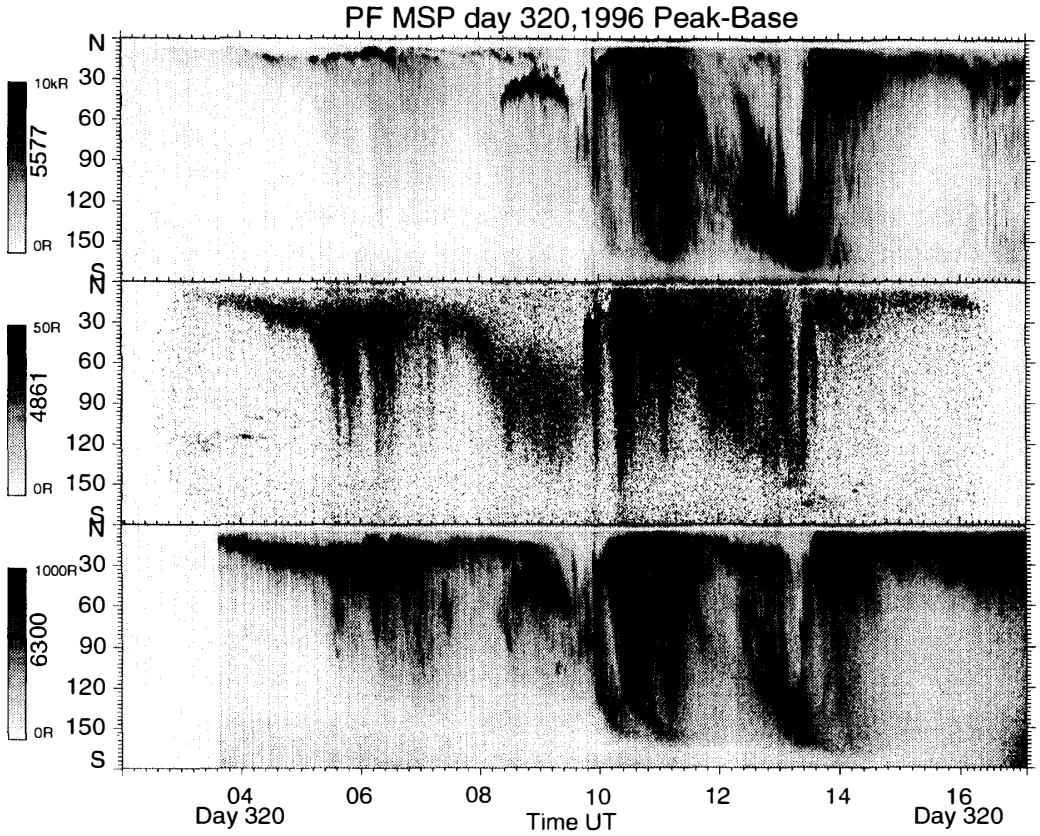

Fig. 2. Poker Flat meridian scanning photometer data for November 15, 1996. These panels indicate airglow and auroral emission intensities at λ557.7 nm (top), λ486.1 nm (middle), and λ630.0 nm (bottom) measured along the magnetic meridian as functions of universal time. The Y-axis indicates viewing angle in degrees along the magnetic meridian, with 0 corresponding to the north horizon and 180 to the south horizon. The intensity scale is linear, with black corresponding intensities of at least 10000, 50, and 1000 Rayleighs for the top, middle and bottom panels respectively.

ASI-FPS only viewed about 130° full-angle. However, the geographic regions viewed by the two instruments corresponded more closely than might be expected based solely on their angular fields-of-view. This is because the emissions viewed by the ASC typically originate at a lower altitude than the λ630 nm emission viewed by the ASI-FPS.

Figure 1 shows the evolution of the thermospheric horizontal wind field throughout the night, while Fig. 2 shows the MSP auroral record. Prior to about 1000 UT, the aurora lay north of Poker Flat, moving gradually southward with time. A breakup began just before 1000 UT, so that there was active aurora over much of the sky until about 1400 UT, when the arcs reformed in the north and remained there for the rest of the night.

The wind blew uniformly northeastward early in the night. Such flow is expected at this time; it corresponds to the approximately antisunward flow driven by the pressure gradient established by solar heating. As the evening advanced, the uniform flow became curved and sheared with respect to latitude, so that equatorward of Poker Flat the wind blew toward the east, whereas poleward of the observatory it blew toward the west.

High spatial resolution thermospheric models predict that a "channel" of locally enhanced zonal winds should occur within a latitudinal band several hundred kilometers wide running along a stable auroral arc (ST.-MAURICE and SCHUNK, 1981; FULLER-ROWELL, 1985; LYONS and WALTERSCHEID, 1985; WALTERSCHEID *et al.*, 1985; CHANG and ST.-MAURICE, 1991; WALTERSCHEID and LYONS, 1992; KESKINEN and SATYANARAYANA, 1993). The models suggest that the zonal wind stream can reach speeds of several hundred ms^{-1}. It would blow westward prior to magnetic midnight, and eastward after magnetic midnight. We thus interpret the observed region of curved and sheared zonal wind as arising due to a transition between eastward pressure-gradient flow and a westward wind stream associated with the stable, pre-breakup auroral arcs seen by the MSP and ASC.

The sheared flow appeared to move equatorward between 0600 and 1000 UT, as did the visible aurora. That is, at 0615 the zonal wind was symmetric about Poker Flat, with opposing flows of similar speed lying due north and due south of it. However, by 1000, the westward flow had moved close to the observatory's zenith, whereas the eastward flow had receeded equatorward and out of the field-of-view. This wind field collapsed within 45 min of the breakup, leaving weak and confused flow over our entire sky.

At 1045 (an hour after the breakup), the cross-polar jet entered our field-of-view, appearing as southeastward flow in the viewing zones lying furthest north and northeast of the observatory. The appearance of the jet was delineated by a sharp "front" in the flow; there was a clear distinction between the jet's southeastward flow and the still-stagnant wind field covering the rest of the sky. Over the 90 min or so from 1045 to 1215, the cross-polar jet gradually advanced across our field-of-view, and the delineation between it and the stagnant flow gradually became less abrupt. By 1215 UT uniform southeastward flow appeared across the whole sky.

Figure 3 presents a compilation of data from the four instruments over a three hour period around the time of the breakup. From the top, the time-series show vertical wind, horizontal wind fields, all-sky camera images, and keograms of the MSP data for the λ557.7, λ486.1, and λ630.0 nm channels respectively.

Although not shown in the figure, typical uncertainties associated with the narrow-field FPS vertical wind estimates were $\sim$10 ms^{-1}. The vertical wind accuracy was limited mostly by the etalon's wavelength stability, rather than the signal/noise ratio of the recorded spectra. The gaps in the vertical wind plot arose because the narrow-field FPS was programmed to make a sequence of off-zenith observations after every sixth zenith measurement. These observations were at 60° zenith angle, in azimuths corresponding to geomagnetic north, east, south, and west. We have compared the low-resolution horizontal winds indicated by these off-zenith observations with the higher resolution wind fields obtained from the ASI-FPS; good agreement was found. We also compared the narrow-field FPS vertical wind values to the wind estimates obtained from the central viewing zone of the imaging FPS. Unfortunately, this comparison was not particularly useful because the uncertainties in the imaging FPS winds were too large. (We normally set the imaging FPS integration time to yield typical wind uncertainties of $\sim$20 ms^{-1}, which is acceptable for horizontal winds but too large for vertical winds.)

CONDE and SMITH (1998) considered possible mechanisms for a post-breakup collapse of the horizontal wind, and for the sharp front defining the appearance of the

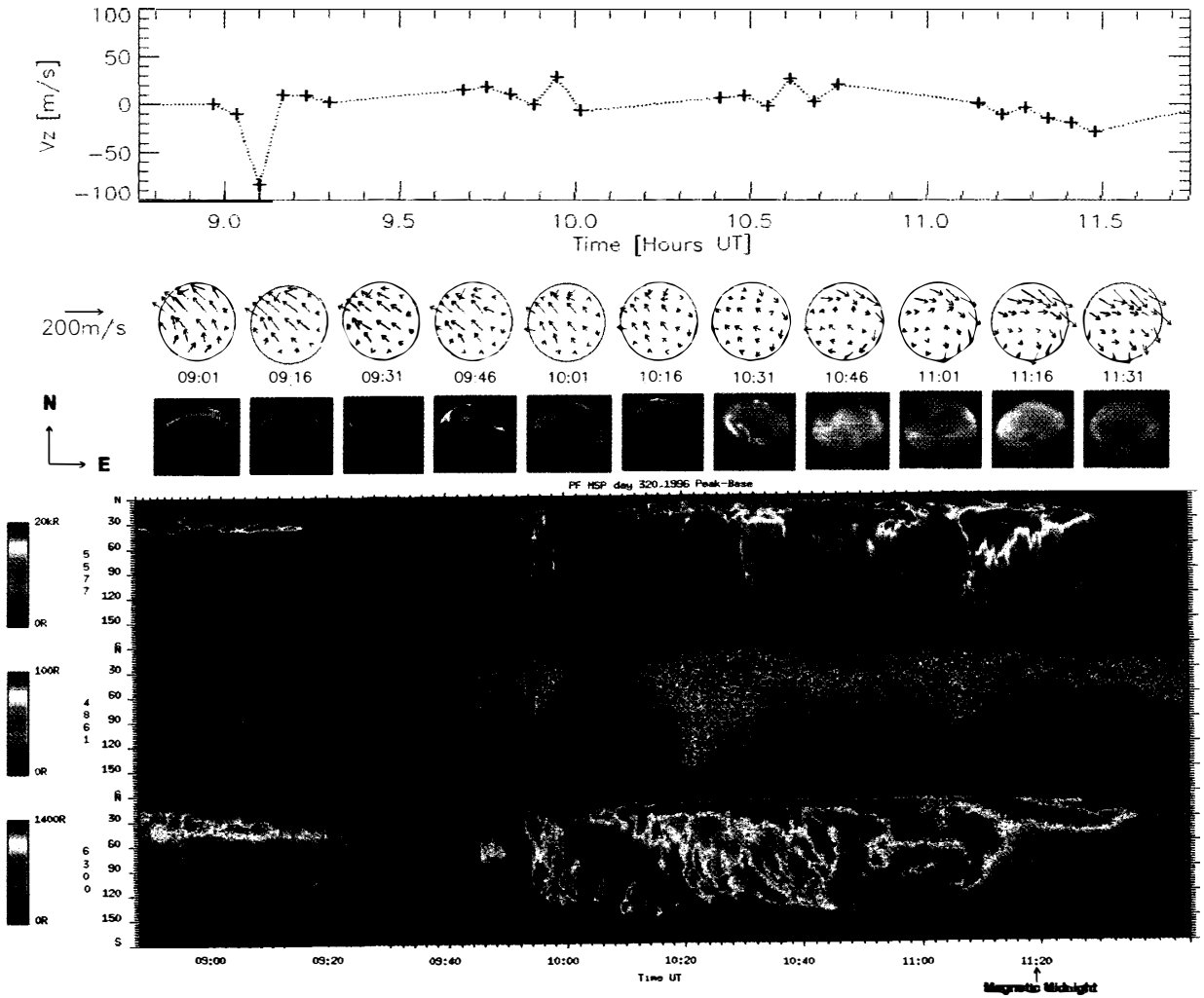

Fig. 3. A compilation of data from the four instruments discussed in the text, over an approximately three hour interval near magnetic mignight on November 15, 1996. From the top, the time series show vertical wind, horizontal wind fields, all-sky camera images, and keograms of the MSP data for the λ557.7, λ486.1, and λ630.0 nm channels respectively. Color bars indicate the MSP intensity scale in each channel. Magnetic midnight is indicated on the MSP time axis.

cross-polar jet. They suggested that vertical winds associated with the auroral oval in general, and with an auroral breakup in particular, may act through vertical advection of horizontal momentum to stagnate the *F*-region flow. The sharp front at the edge of the cross-polar jet could arise in this case due to the jet "running into" the stagnant air mass carried aloft by the vertical wind. Apart from one isolated downward velocity of $-83\ \mathrm{ms}^{-1}$ at 0906 UT, Fig. 3 shows no obvious events in the vertical wind data, and there is no clear correlation with either the horizontal wind or with the aurora. (An upward wind of $30\ \mathrm{ms}^{-1}$ was observed at 0957, close to the time of the auroral breakup, but the significance of this datum is not clear.) Thus, we do not find explicit support in these data for the proposal that upward vertical winds are responsible for stagnating the *F*-region flow. However, as pointed out by CONDE and SMITH (1998), upwelling need not occur in the same location as an observed stagnation, so these data do not exclude the vertical advection hypothesis either.

Statistically, Poker Flat would be expected to have passed under the Harang discontinuity within the time interval spanned by Fig. 3. This passage would be accompanied by a transition from approximately geomagnetic westward *F*-region plasma convection above the observatory to approximately eastward convection. Indeed, the horizontal wind was observed to change from being northwestward at around 0930 UT to southeastward by 1200. Thus, the observed horizontal wind stagnation at around 1030 may simply have been an intermediate state in a transition occurring in response to a rapid reversal of the ion-drag force. The MSP record indicates that although an auroral breakup did commence just prior to 1000, the most energetic particle precipitation (indicated by the $\lambda 558$ keogram) continued to occur well north of Poker Flat. If this also corresponded to region of greatest auroral ionization rate, then the time constant for ion-neutral momentum coupling would have been shortest to the north of our observatory. Thus, the sharp front observed in the horizontal wind may have arisen because the wind field was able to follow the plasma reversal more rapidly near the (sharply defined) regions of energetic auroral precipitation.

Without additional instrumentation, we cannot determine the extent to which either or both of these mechanisms contributed to the final, observed wind field. Testing the vertical advection hypothesis would require adding a north-south array of at least three instruments measuring vertical winds. Testing the hypothesis of aurorally modulated ion-neutral momentum coupling would require observations over interior Alaska using either an incoherent scatter radar or a two station superDARN radar array. Fortunately, current instrumentation proposals may see some or all of these new facilities established in Alaska before the next solar maximum.

4. Conclusions

We have presented a compilation of data from two instruments measuring thermospheric winds and two instruments monitoring the aurora. These data were obtained on the night of November 15, 1996, from Poker Flat, Alaska. Visual comparison of these data sets suggests a close association between the aurora and spatial structure in the horizontal vector wind fields. In particular, the location and latitudinal movement of a region of sheared zonal wind in the late evening hours closely followed that of auroral

arcs observed prior to a breakup, which commenced just before 1000 UT. Within 45 min of the breakup, the sheared flow collapsed, leaving weak and confused winds. Following this, the cross-polar jet was observed to move into our field-of-view, with a sharp "front" in the horizontal flow delineating its edge. Even during the breakup, the most energetic auroral precipitation occured north of Poker Flat. A possible explanation for the sharpness of the edge of the cross-polar jet is that this precipitation formed a well-defined region where the time constant for ion-neutral momentum coupling was reduced relative to its value further south. Thus, in this region to the north of Poker Flat, the wind field may have been able to adjust itself more rapidly to the expected reversal of the direction of the ion-drag force as our observatory passed under the Harang discontinuity. An alternate possibility is that the auroral breakup may have carried horizontally sluggish air aloft, stagnating the flow at *F*-region heights. The sharply defined edge of the cross-polar jet could have arisen as the jet collided with this stagnant air mass. Simultaneous vertical wind observations do not support the upwelling hypothesis. However, they do not exclude it either.

Acknowledgments

We would like to thank June PELEHOWSKI for her assistance with the operation of both Fabry-Perot spectrometers, the MSP, the ASC, and the laboratory at Poker Flat. We would also like to thank Tom HALLINAN and Edward HOCH for providing the all-sky camera data. IMF data for November 15, 1996, was obtained from the "cdaweb" world-wide-web service, at the URL

http://cdaweb.gsfc.nasa.gov/cdaweb/istp_public/

One of us (M.C.) gratefully acknowledges the invitation of the Japanese National Institute of Polar Research to visit Japan and to present this work.

References

BATES, H. F. and ROBERTS T. D. (1977): The southward midnight surge in F-layer wind observed with the Chatanika incoherent scatter radar. J. Atmos. Terr. Phys., **39**, 87–93.

CHANG, C. A. and ST.-MAURICE, J.-P. (1991): Two-dimensional high-latitude thermospheric modeling: a comparison between moderate and extremely disturbed conditions. Can. J. Phys., **69**, 1007–1031.

CONDE, M. and SMITH, R. W. (1997): "Phase compensation" of a separation scanned, all-sky imaging Fabry-Perot spectrometer for auroral studies. Appl. Opt., **36**, 5441–5450.

CONDE, M. and SMITH, R. W. (1998): Spatial structure in the thermospheric horizontal wind above Poker Flat, Alaska, during solar minimum. J. Geophys. Res., **103**, 9449–9472.

FULLER-ROWELL, T. J. (1985): A two-dimensional, high-resolution, nested-grid model of the thermosphere 2. Response of the thermosphere to narrow and broad electrodynamic features. J. Geophys. Res., **90**, 6567–6586.

HAYS, P. B., MERIWETHER, J. W., Jr. and ROBLE, R. G. (1979): Nighttime thermospheric winds at high latitudes. J. Geophys. Res., **84**, 1905–1913.

HAYS, P. B., KILLEEN, T. L., SPENCER, N. W., WHARTON, L. E., ROBLE, R. G., EMERY, B. A., FULLER-ROWELL, T. J., REES, D., FRANK, L. A. and CRAVEN, J. D. (1984): Observations of the dynamics of the polar thermosphere. J. Geophys. Res., **89**, 5597–5612.

HEPPNER, J. P. and MILLER, M. L. (1982): Thermospheric winds at high latitudes from chemical release observations. J. Geophys. Res., **87**, 1633–1647.

KESKINEN, M. J. and SATYANARAYANA, P. (1993): Nonlinear unstable auroral-arc driven thermospheric

winds in an ionosphere-magnetosphere coupled model. Geophys. Res. Lett., **20**, 2687–2690.

KILLEEN, T. L. and ROBLE, R. G. (1988): Thermosphere dynamics: contributions from the first 5 years of the Dynamics Explorer program. Rev. Geophys., **26**, 329–367.

KILLEEN, T. L., CRAVEN, J. D., FRANK, L. A., PONTHIEU, J.-J., SPENCER, N. W., HEELIS, R. A., BRACE, L. H., ROBLE, R. G., HAYS, P. B. and CARIGNAN, G. R. (1988): On the relationship between dynamics of the polar thermosphere and morphology of the aurora: Global-scale observations from Dynamics Explorers 1 and 2. J. Geophys. Res., **93**, 2675–2692.

LARSEN, M. F., MARSHALL, T. R., MIKKELSEN, I. S., EMERY, B. A., CHRISTENSEN, A., KAYSER, D., HECHT, J., LYONS, L. and WALTERSCHIED, R. (1995): Atmospheric response in aurora experiment: Observations of *E* and *F* region neutral winds in a region of postmidnight diffuse aurora. J. Geophys. Res., **100**, 17299–17308.

LARSEN, M. F., CHRISTENSEN, A. B. and ODOM, C. D. (1997): Observations of unstable atmospheric shear layers in the lower E region in the post-midnight auroral oval. Geophys. Res. Lett., **24**, 1915–1918.

LYONS, L. R. and WALTERSCHEID, R. L. (1985): Generation of auroral omega bands by shear instability of the neutral winds. J. Geophys. Res., **90**, 12321–12329.

MERIWETHER, J. W., Jr., HEPPNER, J. P., STOLARIK, J. D. and WESCOTT, E. M. (1973): Neutral winds above 200 km at high latitudes. J. Geophys. Res., **78**, 6643–6661.

MIKKELSEN, I. S., JØRGENSEN, T. S., KELLEY, M. C., LARSEN, M. F., PEREIRA, E. and VICKREY, J. (1981): Neutral winds and electric fields in the dusk auroral oval 1. Measurements. J. Geophys. Res., **86**, 1513–1524.

NAGY, A. F., CICERONE, R. J., HAYS, P. B., MCWATTERS, K. D., MERIWETHER, J. W., Jr., BELON, A. E. and RINO, C. L. (1974): Simultaneous measurements of ion and neutral motions by radar and optical techniques. Radio Sci., **9**, 315–321.

SICA, R. J., REES, M. H., ROMICK, G. J., HERNANDEZ, G. and ROBLE, R.G. (1986): Auroral zone thermospheric Dynamics 1. Averages. J. Geophys. Res., **91**, 3231–3244.

SICA, R. J., HERNANDEZ, G., EMERY, B. A., ROBLE, R. G., SMITH, R. W. and REES, M. H. (1989): The control of auroral zone dynamics and thermodynamics by the interplanetary magnetic field dawn-dusk (Y) component. J. Geophys. Res., **94**, 11921–11932.

SICA, R. J., ST.-MAURICE, J.-P., HERNANDEZ, G., ROMICK, G. J. and TSUNODA, R. (1993): Computations of local ion energy balance in the auroral zone. J. Geophys. Res., **98**, 15667–15676.

SMITH, R. W., MERIWETHER, J. W., Jr., HERNANDEZ, G., REES, D., WICKWAR, V., DE LA BEAUJARDIERE, O. and KILLEEN, T. L. (1989): Mapping the wind in the polar thermosphere: A case study within the CEDAR Program. Eos, **70**, 161.

SPENCER, N. W., WHARTON, L. E., CARNIGAN, G. R. and MAURER, J. C. (1982): Thermosphere zonal winds, vertical motions and temperature as measured from Dynamics Explorer. Geophys. Res. Lett., **9**, 953–956.

ST.-MAURICE, J.-P. and SCHUNK, R. W. (1981): Ion-neutral momentum coupling near discrete high-latitude ionospheric features. J. Geophys. Res., **86**, 11299–11321.

WALTERSCHEID, R. L. and LYONS, L. R. (1992): The neutral circulation in the vicinity of a stable auroral arc. J. Geophys. Res., **97**, 19489–19499.

WALTERSCHEID, R. L., LYONS, L. R. and TAYLOR, K. E. (1985): The perturbed neutral circulation in the vicinity of a symmetric stable auroral arc. J. Geophys. Res., **90**, 12235–12248.

WICKWAR, V. B., MERIWETHER. J. W., HAYS, P. B. and NAGY, A. F. (1984): The meridional thermospheric neutral wind measured by radar and optical techniques in the auroral region. J. Geophys. Res., **89**, 10987–10998.

(Received August 28, 1997; Revised manuscript accepted June 2, 1998)